

Mass dependence of positive pion-induced fission

H. A. Khan

*Solid State Nuclear Track Detector Laboratory, Nuclear Engineering Division,
Pakistan Institute of Nuclear Science and Technology, P.O. Nilore, Islamabad, Pakistan*

N. A. Khan

COMSTECH, Islamabad, Pakistan

R. J. Peterson

Nuclear Physics Laboratory, University of Colorado, Boulder, Colorado 80309

(Received 27 April 1990)

Fission cross sections for a range of targets have been measured by solid-state track detectors following 80 and 100 MeV π^+ bombardment. Fission probabilities have been inferred by comparison to computed reaction cross sections. Fission probabilities for heavy targets agree with those for other probes of comparable energy and with statistical calculations. Probabilities for lighter targets are much above those previously observed or computed. Ternary fission cross sections and multiplicities of light fragments have also been determined.

I. INTRODUCTION

Sparse data for pion-induced fission have been compared to calculations and results of other energetic beams, and it is remarkable to note that for the same initial excitation energy, fission probabilities are similar for each probe with targets $A \geq 197$.¹ For lighter nuclear targets, fission is less likely and the lowering of the fission barrier by angular momentum will have a strong effect on fission probabilities, as familiar from fission by heavy-ion beams.² In this work we greatly extend the range of targets for positive pion-induced fission from the targets considered in Ref. 1, which uses the results of Hicks *et al.*³ The range of target masses is nearly as large as that considered for 190-MeV proton-induced fission in Ref. 4. We find larger fission probabilities for lighter nuclei than is predicted with methods successful for heavier nuclei.¹ Together with results of Ref. 5, we also provide a demonstration that 80- and 100-MeV π^+ beams yield very similar fission cross sections. In order to compare to fission due to stopped π^- ,⁶ we compute fission probabilities for π^+ by comparison to reaction cross sections computed by a pion optical model.

Beam energies of 80 and 100 MeV were chosen to enhance the probability of true pion absorption, in order to gain the rest mass energy of the projectile. For Bi the π^+ absorption cross section is maximum and flat at these energies, becoming about 60% of the reaction cross section, the sum of observed inelastic, charge exchange, and absorption cross sections.⁷

II. METHODS AND RESULTS

Positive pion beams of 80 and 100 MeV from the LEP beam line at LAMPF (Los Alamos) were used as for the results of Hicks *et al.*³ Just outside the vacuum chamber, stacks of fission targets and track detector materials were placed in the beam. Results of these expo-

surements have been reported in Ref. 5 for some target materials. Development and scanning for the work reported here have followed the same methods as in Refs. 5 and 8. Spectroscopically pure Th, Bi, W, and Hf were deposited with thicknesses between 300 and 1150 $\mu\text{g}/\text{cm}^2$ on seven types of solid-state nuclear track detectors with a wide range of thresholds in Z and Z/β . Target thicknesses were known to better than 7%. With mica as a front detector for heavy fragments, CR-39 behind the mica was used to register both light and heavy fragments on both sides of the target material. The highest energy for which a charged particle can produce an etchable latent damage trail under the present experimental conditions for protons was about 5 MeV and for alpha particles was about 19 MeV.

Binary fission was defined by two back-to-back events in the mica sheets with each track due to a fragment of at least $Z=16$ and mass 32. Pion beam normalization was carried out by an activation process as before,⁵ with an uncertainty of 20%. This is not included in the uncertainties for individual targets. Two stacks of foils and detectors were used, for 80- and 100-MeV beams, and all results from each stack were obtained by the same methods. Results are listed in Table I, together with those for U, Pb, and Au from Ref. 5 from the same exposures. Where comparisons can be made, good agreement is found with the work of Hicks *et al.*³

Ternary fission events were observed as three correlated tracks. Cross sections are listed with those from Ref. 5 in Table II.

Long-range products ($Z \leq 8$) were also observed in the CR-39 to be associated with fission tracks in mica, with fewer light products per fission event for the lighter targets. For thorium at 80 MeV, more than 90% of the light products are protons and alpha particles, with less than 8% of the total having $2 < Z \leq 8$. The angular correlation between fission tracks and light products is nearly isotropic. If fitted by the form

TABLE I. Binary fission cross sections in mb and fission probabilities for π^+ on several targets. Fission probabilities are obtained by comparing fission cross sections to computed reaction cross sections.

	80 MeV		100 MeV	
	σ_f	W_f	σ_f	W_f
^{238}U	2020 ± 45^a	1.037		
^{232}Th	1830 ± 41	0.952	1989 ± 45	1.00
^{209}Bi	310 ± 19	0.167	332 ± 20	0.173
$^{207,2}\text{Pb}$	260 ± 17^a	0.141	258 ± 16^a	0.134
^{197}Au	79 ± 9^a	0.045	81 ± 9^a	0.044
$^{183,9}\text{W}$	22 ± 5	0.012	21 ± 5	0.011
$^{178,5}\text{Hf}$	7 ± 3	0.0042	8 ± 3	0.0048
^{165}Ho	3 ± 2	0.0018	4 ± 2	0.0023

^aReference 5, analyzing exposures during the same run as for the present data.

$W(\Theta) = A(1 + B\cos^2\Theta)$, the coefficients B are 0.13 (Th), 0.20 (Bi), 0.32 (W), 0.32 (Hf), and 0.33 (Ho). This correlation has previously been noted for 300-MeV positive pions,⁹ where we fitted the data shown to find $B = 1.56 \pm 0.2$. At 80 MeV the ratio of light particles ($Z \leq 8$) to fission events is 2.45 for Th and 1.93 for Hf in the present work.

Fission probabilities were inferred by the ratio of binary fission cross section to computed reaction cross sections. A pion optical model based upon the impulse approximation¹⁰ was used, without an energy shift or any

TABLE II. Ternary fission cross sections in mb are listed for two positive pion beam energies.

	80 MeV	100 MeV
^{238}U	11 ± 4^a	
^{232}Th	10 ± 3	10 ± 3
^{209}Bi	2 ± 1	3 ± 1
$^{\text{nat}}\text{Pb}$	1 ± 1^a	
$^{\text{nat}}\text{W}$	1 ± 1	2 ± 1

^aFrom Ref. 5.

second-order parameters. Pion-nucleon phase shifts from Rowe, Salomon, and Landau¹¹ were used, while the geometrical distributions were taken from electron cross-section measurements.¹² Neutron distributions were taken to be identical to proton distributions. The small effect of the nucleon finite size was not included. Computed reaction cross sections and measured fission cross sections give the binary fission probabilities listed in Table I and plotted in Fig. 1 for 80 MeV. The 100-MeV results closely agree with those at 80 MeV, in agreement with the weak beam energy dependence reported in Ref. 3.

Our computed reaction cross sections can be compared with measured values, taken to be the sum of absorption, charge exchange, and inelastic cross sections.⁷ For Fe, Nb, and Bi at 85 and 125 MeV, our calculated reaction cross sections average 75% of those measured (to an ac-

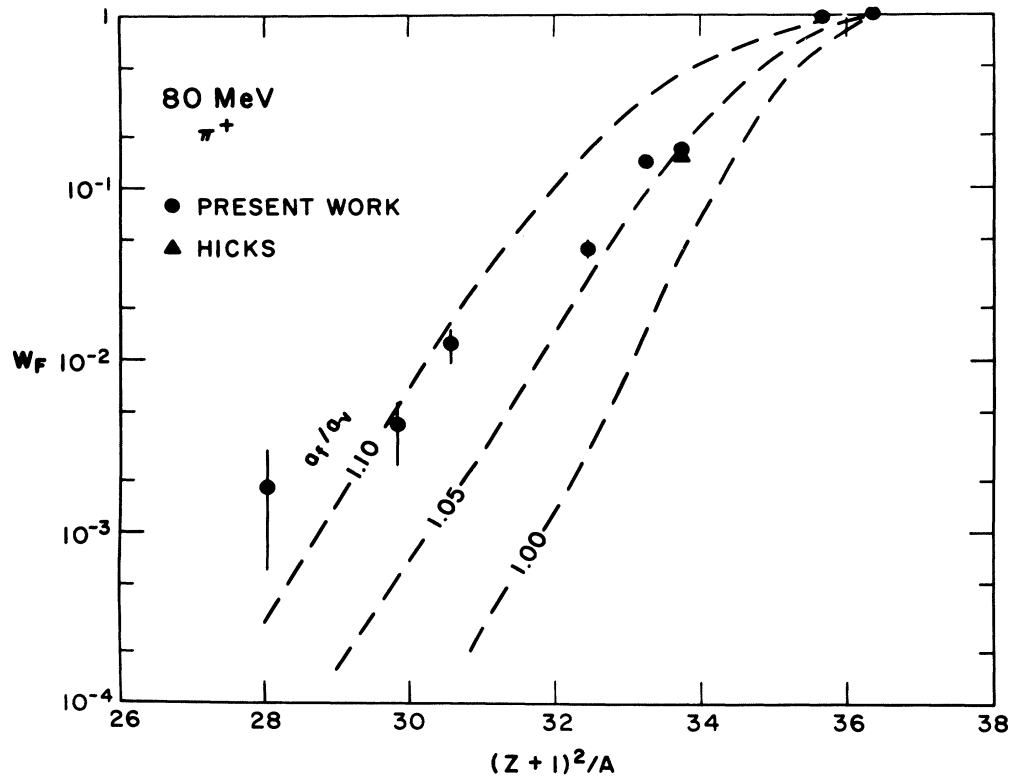


FIG. 1. Fission probabilities from Table I for 80-MeV π^+ are plotted against the fissility parameter for the initial system, $(Z+1)^2/A$, and compared to previous points. Very similar results are observed for 100-MeV π^+ . The dashed curves are those predicted in Ref. 3 for three ratios of level density parameters.

curacy of about 25%), with somewhat better agreement for the lighter targets. If there is a systematic trend with target, this indicates that we infer systematically smaller fission probabilities for the lighter targets than for the heavier.

III. COMPARISONS

Statistical calculations have been carried out for 80-MeV π^+ fission probabilities in Refs. 1 and 3. The curves and 80-MeV data from Ref. 3 are compared to the present results in Fig. 1, where three values of the ratio of fission to neutron level density parameters a are used for the dashed curves. The horizontal axis uses $(Z+1)^2/A$ for the fissility parameter for the initial system. No one curve can match the trend of the data, with a drop below the curve using a ratio of 1.10 near doubly magic lead. A similar drop in W_f is predicted for fission following absorption of stopped π^- , due to ground-state mass-shell effects.¹³

Fission probabilities for stopped π^- are compared to the present 80-MeV π^+ results in Fig. 2, with the middle curve from Ref. 3 repeated for comparison. The π^- data are plotted against $(Z-1)^2/A$, while π^+ data use $(Z+1)^2/A$. These probabilities agree very well with a smooth curve for targets heavier than bismuth. For lighter systems the 80- and 100-MeV π^+ fission probabilities are about 10 times those for stopped pions.

Protons of 190 MeV kinetic energy yield about the same initial excitation as do 80-MeV pions, and so we

compare fission probabilities in Fig. 3 for these beams, with proton data from Ref. 4. The curve uses $a_f/a_v=1.05$ as in Figs. 1 and 2, but is computed for 190-MeV proton-induced fission,⁴ and $(Z+1)^2/A$ is used for the fissility axis. Although the proton data extend to lighter nuclei, over the range treated here for pions the curve agrees quite well with the proton data. Fission probabilities for 80-MeV pions are greater than those for 190-MeV protons and are much higher than those for excitation energies of 76 MeV induced by alpha particles.¹⁴ The beam energy of the pion is clearly not sufficient to account for the high fission probabilities observed, which require also the pion rest mass.

In Ref. 1 plots similar to those shown here use the fissility parameter for the compound nucleus, as obtained from a Monte Carlo intranuclear-cascade calculation. Closer agreement among results measured for different probes is then found than is seen in Fig. 3, where no cascade effects have been included.

IV. CONCLUSIONS

Binary fission cross sections for targets from ¹⁶⁵Ho through ²³⁸U for 80- and 100-MeV π^+ beams have been measured and fission probabilities have been inferred by comparison to computed reaction cross sections. Comparison to statistical theories and fission probabilities due to other beams finds the pion results to be notably larger for lighter targets. If only the heaviest targets, gold and above, are considered, calculations and other data tend to

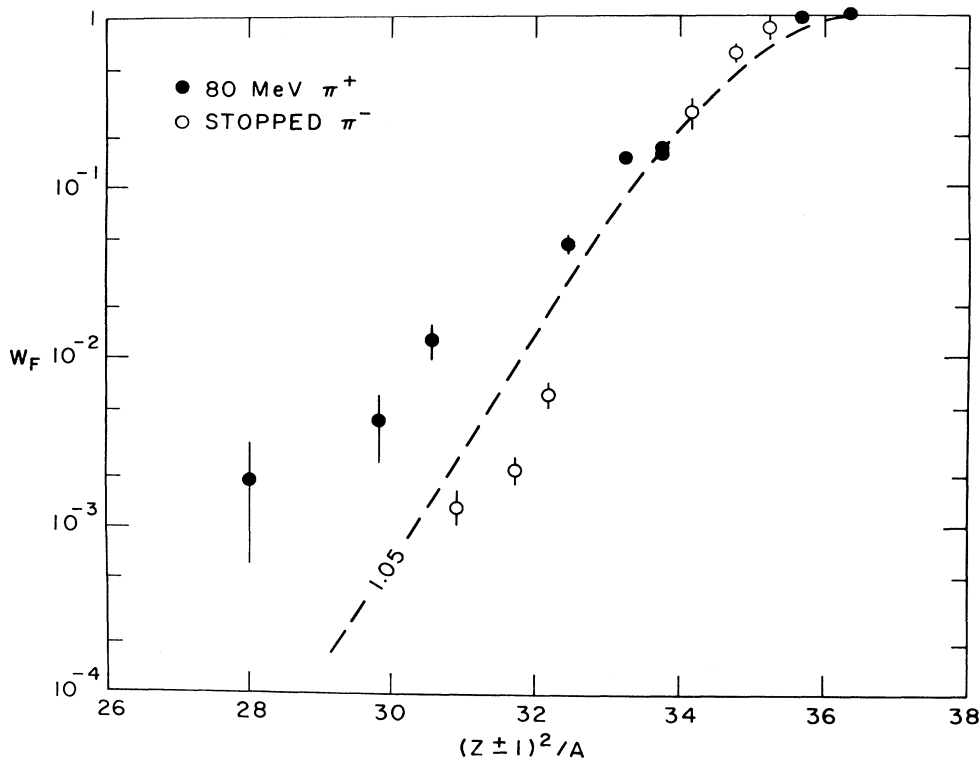


FIG. 2 Fission probabilities and the central dashed curve from Fig. 1 for 80-MeV π^+ are compared to fission probabilities for stopped π^- from Ref. 6. The charge of the initial system is used for the fissility axis, for both beams.

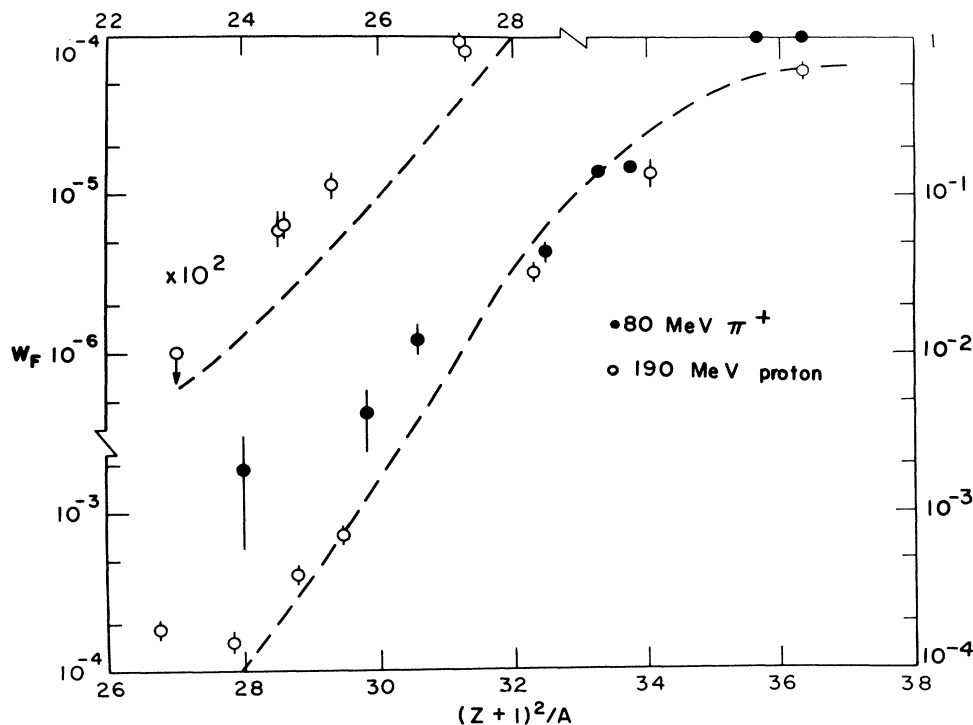


FIG. 3. Fission probabilities from Fig. 1 for 80-MeV π^+ are compared to fission probabilities for 190-MeV protons from Ref. 4. Results for the lightest targets use a different scale. The calculated curve uses $a_f/a_v = 1.05$ as for the central curve in Fig. 1, but is for fission induced by 190-MeV protons, from Ref. 4.

agree with the pion results, as pointed out in Ref. 1. It is for the lighter targets that differences in the probabilities of fission appear as the fission barrier height increases. The interplay between initial excitation energy and angular momentum is demonstrated by the comparison of the present results to data for intermediate-energy protons and stopped π^- . It appears that new forms of calculations will be needed to match the observations for lighter targets.

Further evidence from this work on ternary fission probabilities, multiplicities of light fragments, and angu-

lar correlations between fission products and light fragments can also serve to discriminate among reaction modes. With pion absorption we do seem to have achieved a state of initial high excitation and low angular momentum that evolves into the measured fission probabilities.

This work was supported in part by the International Atomic Energy Agency under IAEA Research Contract No. RBR23455, and in part by the U.S. Department of Energy.

¹A. S. Iljinov *et al.*, Phys. Rev. C **39**, 1420 (1989).

²F. Plasil, T. C. Awes, B. Cheynis, D. Drain, R. L. Ferguson, F. E. Obenshain, A. J. Sierk, S. G. Steadman, and G. R. Young, Phys. Rev. C **29**, 1145 (1984).

³K. H. Hicks *et al.*, Phys. Rev. C **31**, 1323 (1985).

⁴F. D. Becchetti, J. Jänecke, P. Lister, K. Kwiatowski, H. Karwowski, and S. Zhou, Phys. Rev. C **28**, 276 (1983).

⁵H. A. Khan, N. A. Khan, and R. J. Peterson, Phys. Rev. C **35**, 645 (1987).

⁶Y. A. Batusov *et al.*, Yad. Fiz. **23**, 1169 (1976) [Sov. J. Nucl. Phys. **23**, 621 (1976)].

⁷H. J. Pfeiffer and F. H. Schlepütz, Phys. Rev. C **23**, 2173 (1981).

⁸H. A. Khan and N. A. Khan, Phys. Rev. C **29**, 2199 (1984).

⁹G. F. Denisenko, N. S. Ivanova, N. R. Novikova, N. A. Perfilov, E. I. Prokoffieva, and V. P. Shamov, Phys. Rev. C **109**, 1779 (1958).

¹⁰R. A. Eisenstein and G. A. Miller, Comput. Phys. Commun. **11**, 95 (1976).

¹¹G. Rowe, M. Salomon, and R. H. Landau, Phys. Rev. C **18**, 584 (1978).

¹²H. deVries, C. W. deJager, and C. deVries, At. Data Nucl. Data Tables **36**, 495 (1987).

¹³E. Gadioli, E. Gadioli-Erba, and A. Moroni, Z. Phys. A **228**, 39 (1978).

¹⁴R. Vandenbosch and J. R. Huizenga, *Nuclear Fission* (Academic, New York, 1973), p. 217.